
EFDA–JET–CP(07)03/43

G.M.D. Hogeweyj, P. Buratti, J. Brzozowski, R. de Angelis, E. de la Luna,
J. Hobirk, F. Imbeaux, P. Orsitto, I. Voitsekhovitch, K.-D. Zastrow
and JET EFDA contributors

Electron Heated Hybrid JET Discharges: Experimental Results and Modeling

"This document is intended for publication in the open literature. It is made available on the understanding that it may not be further circulated and extracts or references may not be published prior to publication of the original when applicable, or without the consent of the Publications Officer, EFDA, Culham Science Centre, Abingdon, Oxon, OX14 3DB, UK."

"Enquiries about Copyright and reproduction should be addressed to the Publications Officer, EFDA, Culham Science Centre, Abingdon, Oxon, OX14 3DB, UK."

Electron Heated Hybrid JET Discharges: Experimental Results and Modeling

G.M.D. Hogeweyj¹, P. Buratti², J. Brzozowski³, R. de Angelis², E. de la Luna⁴,
J. Hobirk⁵, F. Imbeaux⁶, P. Orsitto², I. Voitsekhovitch⁷, K.-D. Zastrow⁷,
and JET EFDA contributors*

Preprint of Paper to be submitted for publication in Proceedings of the
34th EPS Conference on Plasma Physics,
(Warsaw, Poland 2nd - 6th July 2007)

1. INTRODUCTION.

Tokamak discharges in the hybrid scenario, with a wide area of low magnetic shear (s) and central safety factor (q) close to one, have shown improved MHD stability at high β [1]. Realization of hybrid scenarios with predominant electron heating is a significant step towards ITER-relevant conditions. Such hybrid regimes, with $T_e > T_i$, were first obtained in 2004 in JET; however, they were poorly diagnosed. Recently, these experiments were repeated and extended, with all diagnostics available. After a review of the experiments, this paper presents modeling results, and a comparison with the standard (ion heated) hybrid scenario.

2. EXPERIMENTAL RESULTS.

Hybrid regimes with $T_e > T_i$ have been obtained in JET by means of Ion Cyclotron Resonance Heating (ICRH, frequency 51.7 MHz) with low-concentration hydrogen minority in deuterium plasmas. Hybrid current profiles were formed by Lower Hybrid Current Drive (LHCD) prelude and by adjusting the timing of main heating during the current ramp.

Figure 1 shows the time evolution of reference Pulse No: 68383. Main heating consisted of 9MW neutral beam injection (P_{nbi}) plus 8.5MW ICRH, yielding peak temperatures $T_e = 9-11\text{keV}$ and $T_i = 7-8\text{keV}$, and central toroidal rotation of 30krad/s, at lineaveraged density $2.2 \cdot 10^{19} \text{ m}^{-3}$, corresponding to 0.28 times the Greenwald limit (n_G). The confinement regime was H-mode with H89 up to 2 and $\beta_N \approx 1.5$.

Starting from this reference pulse, other pulses were made by modifying one parameter: (i) a high density pulse with $n_e = 0.57 \cdot n_G$; (ii) a pulse with LH preheat ramped up to 1MW; (iii) two pulses with P_{nbi} up to 16 MW.

The reference LHCD power was 0.7 MW; with this, tiny sawteeth typically developed after 6 s of main heating. Sawteeth were completely suppressed by ramping the LHCD power to 1 MW; however, in this case a persistent $n = 1$ mode developed [2], see Fig.2. The ELM behaviour depended on n_e and input power: whereas the reference pulse had very frequent, tiny ELMs, the high n_e pulse had small, regular ELMs ($f \sim 100\text{Hz}$), and the high power pulses developed ELM-free periods followed by big ELMs.

3. INTERPRETATIVE AND PREDICTIVE MODELING

CRONOS [3] was used both for interpretative and predictive modeling. For the latter, the empirical Bohm/gyroBohm model [4] was used, without taking $E \times B$ shear into account (due to low rotation, the effect of $E \times B$ shear on turbulence reduction is expected to be small). TRANSP [5] was used for calculation of power deposition of ICRH and NBI. We restrict ourselves to the reference pulse, the high density pulse and the high power pulse.

The ICRH power goes predominantly to the electrons and is well peaked (TRANSP analysis), see fig.3. The NBI power deposition profile is much wider. Altogether, slightly more power goes to the electrons than to the ions.

The results of interpretative and predictive modeling are summarized in figures 4 and 5. The time evolution of $T_e(0)$ is reproduced very well by the Bohm/gyroBohm model (upper panel of Fig.4), whereas $T_i(0)$ is somewhat overestimated, except in the high power case (middle panel). The profiles are compared 6 s after start of the main heating, see Fig.5. The T_e profiles reproduced very well, whereas the T_i profiles are too peaked; the T_i edge pedestal was not modelled.

The discharges start sawtoothing at ~ 14 s. The $q(0)$ evolution as calculated from the experimental profiles, see lower panel of Fig.4, is too fast: it drops below 1 already at ~ 10 s, except in the high power case. The $q(0)$ evolution from the Bohm/gyroBohm modeling is a bit slower than the evolution calculated from the experimental profiles. In the same plots also the $q(0)$ evolution from the equilibrium reconstruction is shown, taking into account constraints from the Motional Stark effect measurements.

4. COMPARISON WITH STANDARD HYBRID SCENARIO

Figures 6, 7 and 8 compare the current reference Pulse No: (68383) with a Pulse No: (62494) in the standard hybrid scenario developed earlier on JET [6], characterized by dominant ion heating (19 MW of NBI and 2MW of ICRH) and $T_i > T_e$.

Pulse No: 62494 had much stronger toroidal rotation (Fig.6d), hence also a stronger E_r and $\omega_{E \times B}$ shearing rate (Fig.7ab; neo-classical v_{pol} was assumed in the calculation). As a very rough measure of the effect of $\omega_{E \times B}$ on turbulence suppression, fig.7c shows $\omega_{E \times B}/\gamma$ where γ is a maximum linear growth rate: around mid radius, it is ~ 0.1 and ~ 0.4 for Pulse No's: 68383 and 62494. So the stronger rotation in Pulse No: 62494 is not sufficient to create an ITB; however, the higher value might cause partial turbulence suppression.

Another factor is the ratio T_i/T_e , which is much larger in the standard hybrid pulse (fig.8a). Formulas for the inverse gradient length $R/L_{T_i,crit}$ for ITG mode turbulence as given by Jenko, Weiland and Romanelli [7,8,9] indicate that $R/L_{T_i,crit}$ increases with increasing T_i/T_e . In two of the formulas $R/L_{T_i,crit}$ increases also with s/q ; however, s/q is not much different for the two pulses (Fig.8b). Indeed $R/L_{T_i,crit}$ is clearly higher for Pulse No: 62494 than for Pulse No: 68383 (Fig.8c).

In the region roughly between 3.4 and 3.7m Pulse No: 62494 indeed has much larger $R/L_{T_i,crit}$, see fig.6c; in this region $R/L_{T_i,crit}$ for both pulses is in satisfactory agreement with the predictive formulas. The region of high $R/L_{T_i,crit}$ of Pulse No: 62494 also coincides with the region of enhanced $\omega_{E \times B}$ shearing rate (fig.7c). It is less clear why $R/L_{T_i,crit}$ for Pulse No: 62494 drops to such a low value inside 3.4m. One explanation might be the low heat flux in the central area due to the wide power deposition of NBI. The χ_i profiles show a behaviour consistent with $\omega_{E \times B}$ and R/L_{T_i} : outside $\rho \simeq 0.4$ it is clearly lower for pulse 62494 (fig.7d).

DISCUSSION

ITER relevant hybrid discharges with $T_e > T_i$ and H-mode factor H89 up to 2 have been obtained in JET. These pulses have been compared with a reference standard (ion heated) hybrid discharge.

Both $\omega_{E \times B}$ and T_i/T_e are significantly larger for the latter pulse. In agreement with this, outside 3.4m the inverse T_i gradient scale length was clearly larger for the ion heated pulse, and χ_i was lower. Apparently, ion thermal confinement is deteriorating when one increases electron heating; this has been seen in other machines as well [10].

The clamping of $q(0)$ to a value ≈ 1 is in contrast with simulations which predict $q(0)$ to drop far below 1. Maybe the effect of NTMs on the q profile, as observed in DIII-D, plays a role in keeping $q(0)$ close to 1 in the experiment [11].

ACKNOWLEDGEMENTS.

This work, supported by the European Communities under the contract of Association between EURATOM/FOM, was carried out within the framework of the European Fusion Programme with financial support from NWO. The views and opinions expressed herein do not necessarily reflect those of the European Commission.

REFERENCES

- [1]. Gormezano C. et al, Plasma Phys. Contr. Fusion **46** (2004) B435
- [2]. Buratti P. et al, this conference
- [3]. Basiuk V. et al, Nucl. Fusion **43** (2003) 822
- [4]. Erba M. et al, Plasma Phys. Contr. Fusion **39** (1997) 261
- [5]. Goldston R.J. et al, J. Comp. Phys. (1981)
- [6]. Joffrin E. et al, Nucl. Fusion **45** (2005) 626
- [7]. Jenko F. et al, Phys. Plasmas **8** (2001) 4096
- [8]. Asp E. et al, Critical gradient response of the Weiland model, submitted
- [8]. Romanelli F. et al, Phys. Fluids B**1** (1989) 1018
- [10]. Casper T.A. et al, Plasma Phys. Contr. Fusion **48** (2006) A35
- [11]. Chu M.S. et al, Proc.21th IAEA (2006) EX/1-5

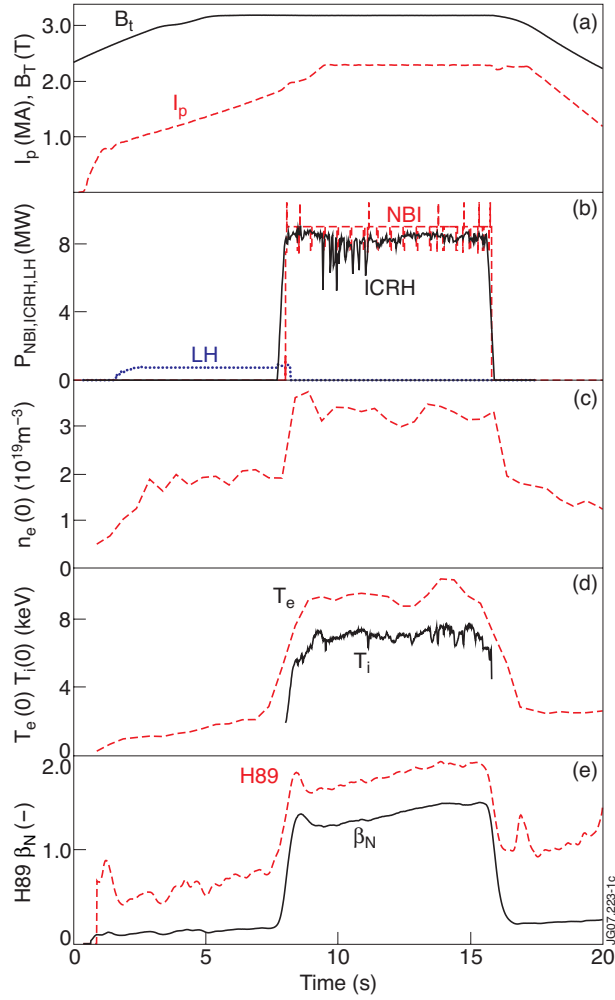


Figure 1: Scenario of reference Pulse No: 68383, showing I_p and B_t (a), LH, ICRH and NBI powers (b), $n_e(0)$ (c), central T_e and T_i (d), H-factor and N (e).

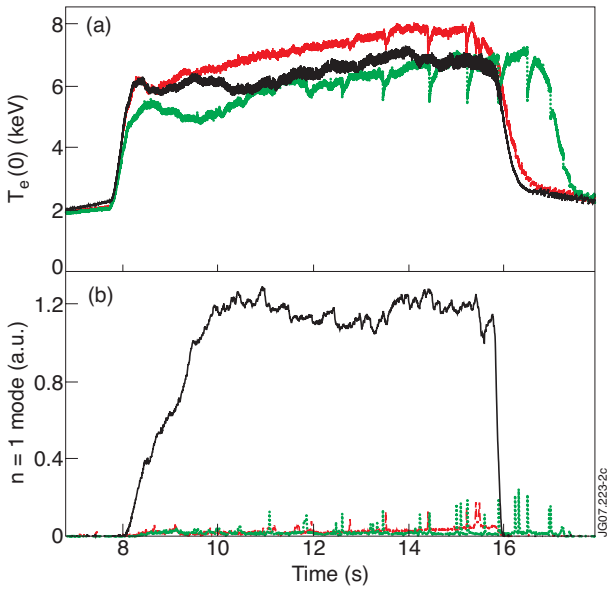


Figure 2: $T_e(0)$ from ECE (a) and $n=1$ mode signal (b) for the reference pulse (red), a pulse with too fast current penetration (green), and one with higher LH preheat (blue).

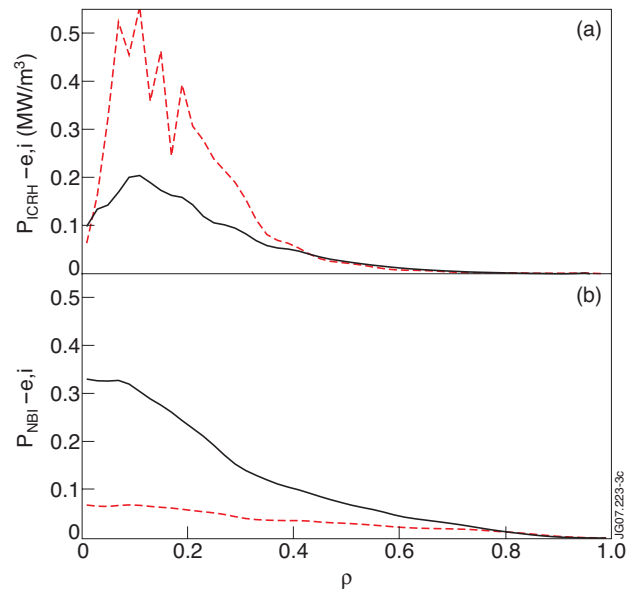


Figure 3: Power density profiles at $t=14s$ of ICRH (a) and NBI (b) to the electrons (red) and ions (blue) for the reference discharge.

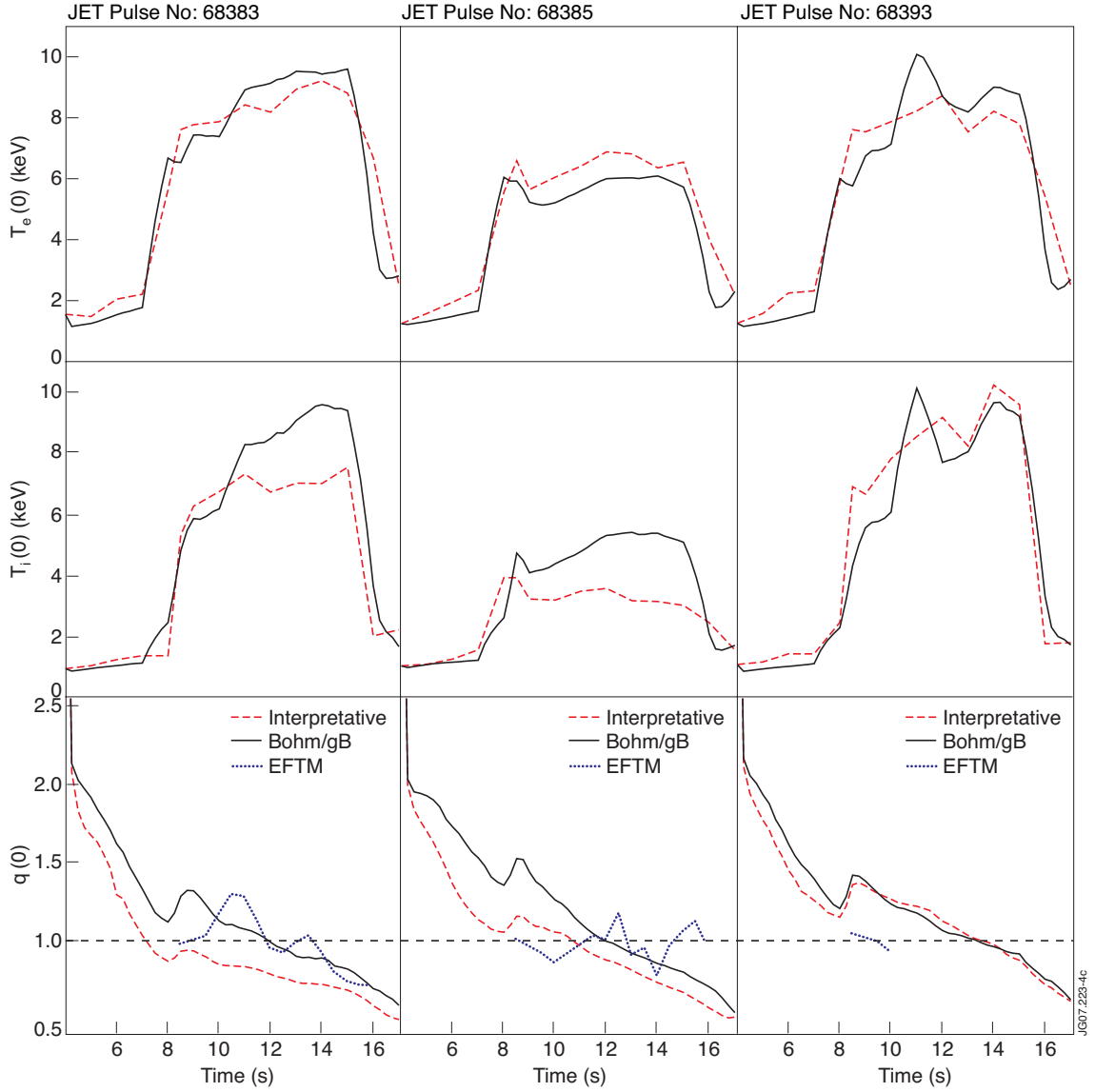


Figure 4: Time traces of central T_e (upper), T_i (middle) and q for the reference discharge (left), high density pulse (middle) and high power pulse (right). Shown are the results of interpretative analysis (red) and predictive modeling with the Bohm/gyroBohm model (green). The lower panels also show the evolution of $q(0)$ from the equilibrium reconstruction using constraints from the MSE measurements (cyan).

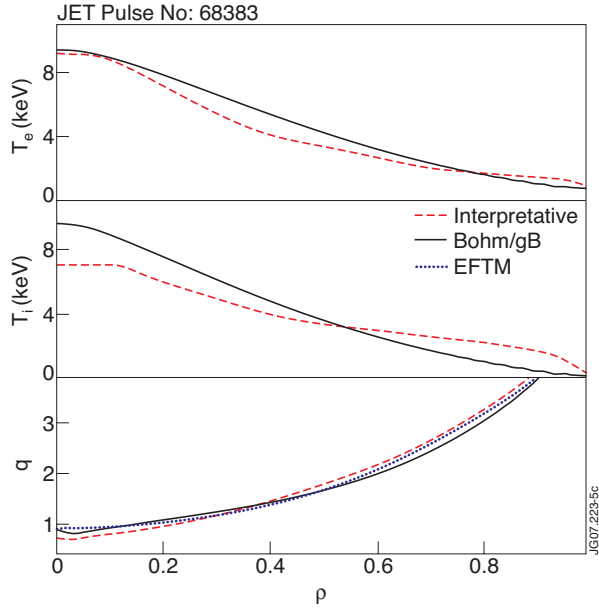


Figure 5: Profiles at $t=14s$ of, from top to bottom, T_e , T_i and q for the same discharges and with the same colour codings as in the previous figure.

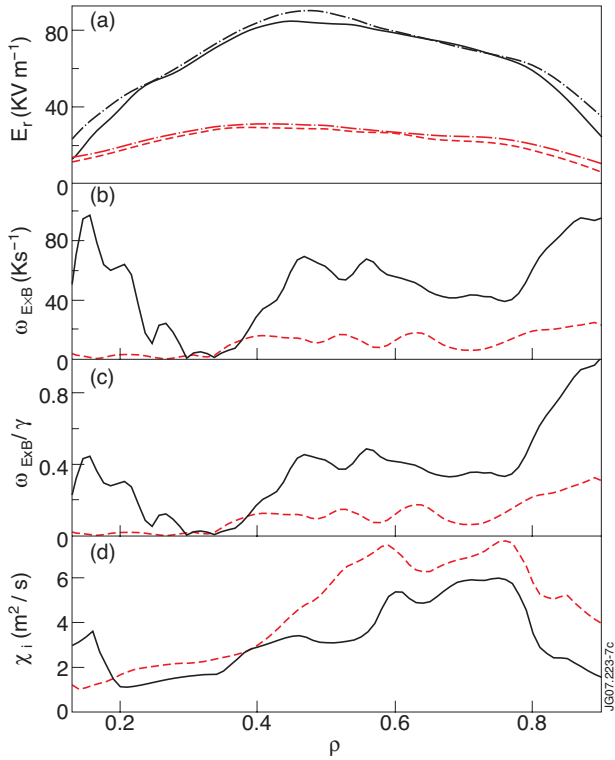


Figure 7: Profiles after 6s of main heating of E_r (a), $\omega_{E \times B}$ (b), and $\omega_{E \times B}/\gamma$ (c), see text), and χ_i (d), for Pulse No's: 68383 (red) and 62494 (blue). In (a) also the contribution to E_r due to the toroidal rotation ($E_{r,\phi}$) is shown (dashed lines).

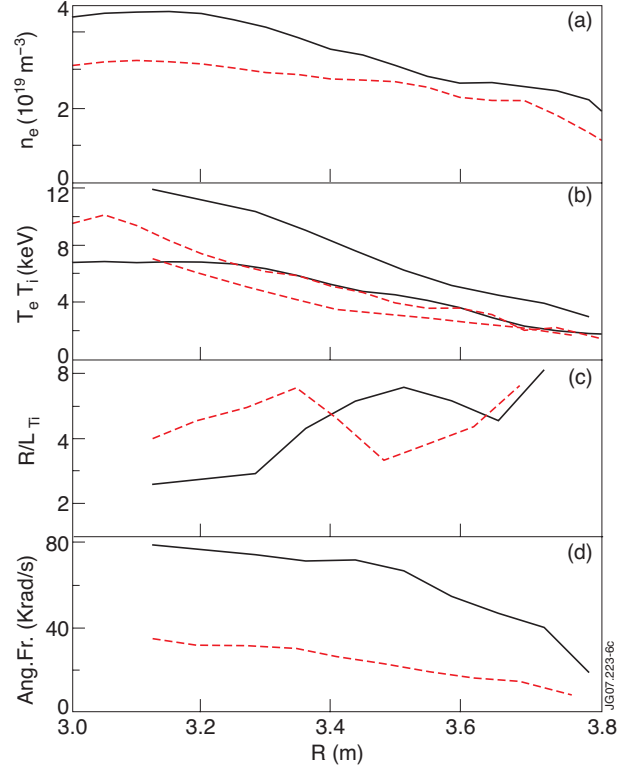


Figure 6: Time averaged profiles during main heating of n_e (a), T_i and T_e (b, full and dashed lines), R/L_{T_i} (c), and toroidal rotation (d), for reference Pulse No: 68383 (red) and the standard ion heated hybrid Pulse No: 62494 (blue).

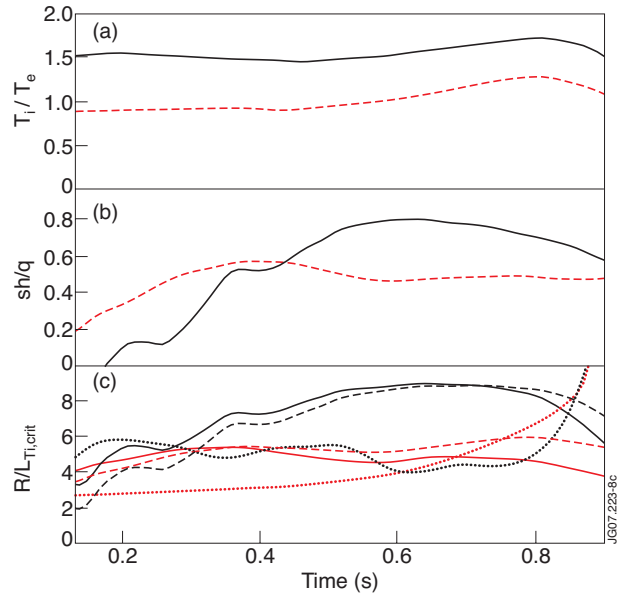


Figure 8: Profiles after 6 s of main heating of T_i/T_e (a), s/q (b) and $R/L_{T_i,crit}$ (c) for pulses 68383 (red) and 62494 (blue). Shown in panel (c) are the expressions of Jenko (full), Weiland (dotted) and Romanelli (dashed, see text).